

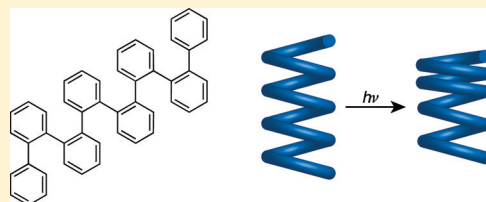
## Excited-State Behavior of *ortho*-Phenylenes

C. Scott Hartley\*

Department of Chemistry & Biochemistry, Miami University, Oxford, Ohio 45056, United States

**S** Supporting Information

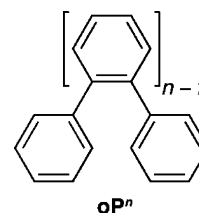
**ABSTRACT:** The excited-state properties of unsubstituted *ortho*-phenylene oligomers have been studied using TD-DFT. Calculations of vertical transitions at the helical ground-state geometries are in good qualitative agreement with the experimental UV–vis spectra. In the excited state, the spring-like compounds compress; for the longer oligomers, this compression is localized at one end of the oligomer. This behavior explains the unusual experimentally observed hypsochromic shifts in fluorescence spectra with increasing oligomer length.



The *ortho*-phenylenes represent a fundamental class of conjugated organic polymers.<sup>1</sup> However, until recently,<sup>2</sup> they have received little attention in the literature compared to the isomeric *meta*- and especially *para*-phenylenes. Unlike most conjugated polymers, they are defined largely by steric strain, which severely attenuates conjugation along their backbones because of poor  $\pi$ -system overlap.<sup>3</sup> Consequently, they tend not to be well-suited to traditional applications of conjugated polymers (e.g., in thin film electronics). However, it has recently been shown that these compounds exhibit well-defined conformational behavior. The *ortho*-phenylenes have therefore begun to attract attention as a new class of helical oligomers.<sup>4–7</sup>

The excited-state behavior of the *ortho*-phenylenes is somewhat unusual. We have reported a series of methoxy-substituted *ortho*-phenylene oligomers that exhibit a reasonably long effective conjugation length of  $n_{\text{ecl}} \approx 8$ , as determined by bathochromic shifts in UV–vis spectra with increasing length;<sup>5</sup> conversely, we have found that the parent (unsubstituted) series **oP<sup>n</sup>** has a much shorter  $n_{\text{ecl}} \approx 4$ .<sup>7,8</sup> This limited delocalization is consistent with the extensive twisting of the *ortho*-phenylene backbone. Remarkably, however, *ortho*-phenylene oligomers exhibit a systematic *hypsochromic* shift in their fluorescence spectra with increasing length; this effect extends over a significantly longer length scale than the changes in UV–vis spectra. To our knowledge, this behavior is unique among simple conjugated polymers<sup>9</sup> and presumably reflects the interplay between conformation and electronic properties for this class of compounds.

To better understand the excited-state behavior of the *ortho*-phenylenes, we undertook a computational investigation of the series of parent oligomers **oP<sup>n</sup>** that we report here. We have found that trends in the spectroscopic properties of these compounds are well-reproduced by TD-DFT methods, allowing the experimental fluorescence shifts to be rationalized by specific excited-state structural changes.



TD-DFT methods have now been extensively applied to the study of conjugated polymers and oligomers,<sup>10</sup> including *para*-phenylenes and related systems.<sup>11–14</sup> After a brief optimization study, we selected the PBE0 functional,<sup>15</sup> using the 6-31+G(d) basis set for all geometry optimizations and the 6-311+G(2d,p) basis set for single-point calculations of energies and electronic transitions. This functional has been successfully used in TD-DFT investigations of *para*-phenylenes,<sup>11</sup>  $\pi$ -stacked systems (e.g., cyclophanes),<sup>16</sup> and dyes in general,<sup>17</sup> suggesting that it would afford at least semiquantitatively accurate results.

Because of the substantial twisting of their backbones, even unsubstituted *ortho*-phenylenes exhibit good solubility in organic solvents (unlike, for example, *para*-phenylenes). Consequently, UV–vis and fluorescence spectra are known for the **oP<sup>n</sup>** series up to the octamer (**oP<sup>8</sup>**),<sup>7</sup> and no groups need to be removed to simplify the structures and reduce computational time. Unfortunately, because of this twisting, the *ortho*-phenylenes exhibit relatively complex conformational behavior in solution, and the different possible conformers differ greatly in the extent of their  $\pi$ -overlap. We have previously shown experimentally that the *ortho*-phenylenes (and the **oP<sup>n</sup>** series specifically) have a strong preference for a compact helical conformer in solution, with an offset stacked relationship between every third repeat unit.<sup>6,7</sup> The few reported solid-state structures of *ortho*-phenylenes are also consistent with this geometry.<sup>2,4,5</sup> We have therefore restricted the present study to this conformational state because it would be impractical to consider every possible conformer, particularly

**Received:** September 6, 2011

**Published:** October 6, 2011

for the excited-state geometry minimizations of the longer oligomers. We note, however, that the real solution-phase conformational behavior of these compounds does deviate from this idealized model, especially at the ends of the chains.<sup>6,7</sup>

Accordingly, we carried out geometry optimizations of the electronic ground states (PBE0/6-31+G(d)) of **oP**<sup>2</sup> (biphenyl), **oP**<sup>3</sup>, **oP**<sup>4</sup>, **oP**<sup>5</sup>, **oP**<sup>6</sup>, and **oP**<sup>8</sup>, with the resulting structures shown in Figures 1 and S1 (Supporting Information). The

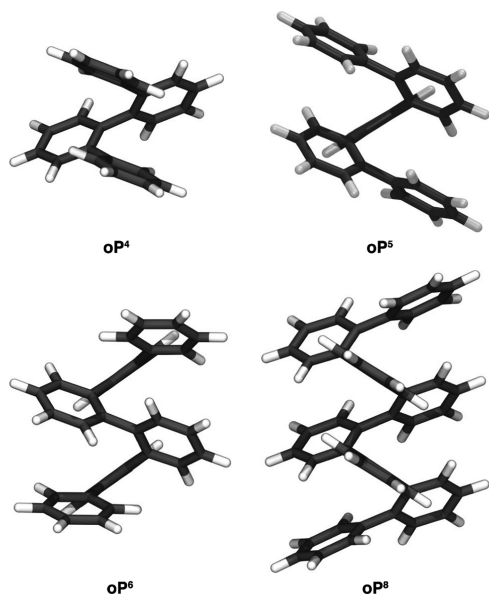


**Figure 1.** Electronic ground-state PBE0/6-31+G(d) geometries of **oP**<sup>4</sup>, **oP**<sup>5</sup>, **oP**<sup>6</sup>, and **oP**<sup>8</sup>.

geometries of the oligomers are  $C_2$ -symmetric (except for **oP**<sup>2</sup>, which is  $D_2$ ). Vertical excitations were then calculated at the TD-PBE0/6-311+G(2d,p) level; in order to capture the low energy absorption behavior of the compounds, 24 excitations were calculated for **oP**<sup>3</sup> and **oP**<sup>4</sup> and 48 for the longer oligomers. Spectra simulated from the calculated transition energies and oscillator strengths show a good qualitative agreement with the experimental absorption spectra in cyclohexane<sup>7</sup> (see Figure S2, Supporting Information). In all cases, the first excitations correspond largely to direct HOMO–LUMO transitions (see Table S1 for energies, oscillator strengths, and compositions and Figure S1 for MOs in the Supporting Information). The oscillator strengths ( $f$ ) for these lowest-energy transitions fall sharply from **oP**<sup>4</sup> ( $f = 0.09$ ) to **oP**<sup>5</sup> ( $f = 0.008$ ) and are small (but nonzero) for the longer oligomers. Unlike **oP**<sup>3</sup> and **oP**<sup>4</sup>, the HOMOs and LUMOs of **oP**<sup>5</sup>, **oP**<sup>6</sup>, and **oP**<sup>8</sup> (all  $C_2$ ) have the same symmetries (i.e., both  $a$  or both  $b$ , Figure S1, Supporting Information). Consequently, the transition dipoles for the HOMO–LUMO excitations of these compounds are polarized along the short axes of the helices, with correspondingly limited  $\pi$ -overlap.

A plot of the first excitation wavelengths ( $\lambda_{n,UV}$ ) against oligomer length ( $n$ ) is given in Figure 2a. As developed by Meier, the UV–vis data can be fit to an empirical equation:<sup>18</sup>

$$\lambda_{n,UV} = \lambda_{\infty,UV} - \Delta\lambda_{UV}e^{-b(n-1)} \quad (1)$$

where  $\lambda_{\infty,UV}$  is the extrapolation of  $\lambda_{n,UV}$  to the polymer limit,  $\Delta\lambda_{UV}$  represents the effect of conjugation (i.e., total shift in  $\lambda_{\infty,UV}$  from monomer to polymer), and  $b$  is the extent of conjugation (i.e., the rate at which  $\lambda_{\infty,UV}$  is approached as  $n$

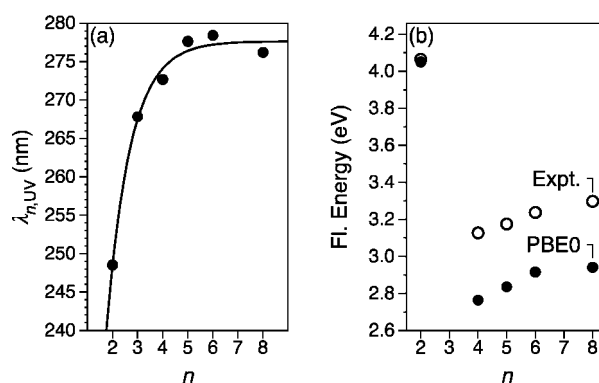


**Figure 2.** (a) Calculated lowest-energy excitation wavelengths vs  $n$  ( $S_0$  state geometry). The solid line is a fit to eq 1, which yields  $\lambda_{\infty,UV} = 277.6 \pm 1.1$  nm,  $\Delta\lambda_{UV} = 83 \pm 14$  nm, and  $b = 1.05 \pm 0.17$ . (b) Calculated and experimental (cyclohexane) fluorescence energies ( $S_1$  state geometry).

increases). From these parameters, the effective conjugation length ( $n_{\text{ecl}}$ ) can be calculated to allow comparison between different conjugated systems. It is defined as the value of  $n$  for which  $\lambda_{\infty,UV} - \lambda_{n,UV} \leq 1$  nm; thus,

$$n_{\text{ecl}} = \frac{\ln\Delta\lambda_{UV}}{b} + 1 \quad (2)$$

From the fit in Figure 2a,<sup>19</sup>  $n_{\text{ecl}} \approx 5$ , which is in good agreement with the experimentally determined  $n_{\text{ecl}} \approx 4$ .<sup>7</sup> The TD-DFT calculations therefore appear to accurately capture delocalization in the weakly conjugated *ortho*-phenylenes, despite their known tendency to overestimate the conjugation length in other conjugated polymers.<sup>10,20</sup>

Encouraged by the agreement between the calculated and experimental UV–vis spectra, we then proceeded to optimize the geometries of the  $S_1$  states for all the oligomers at the TD-PBE0/6-31+G(d) level (except for **oP**<sup>3</sup>, for which experimental data are not available as it is nonfluorescent<sup>21</sup>). Optimized geometries and frontier molecular orbitals are shown in Figure S3 (Supporting Information). The calculated (gas-phase) fluorescence energies (TD-PBE0/6-311+G(2d,p)) underestimate the experimental energies by roughly 0.35 eV for  $n \geq 4$ , as shown in Figure 2b. However, the overall trend, increasing fluorescence energy with increasing length, is in excellent agreement with experiment. For example, the change in fluorescence energy from **oP**<sup>4</sup> to **oP**<sup>8</sup> is 0.18 eV (in the gas phase), compared to the experimental value of 0.17 eV (in cyclohexane). The fluorescence transitions correspond to a direct transition between the  $S_1$  state SOMOs (i.e., electronic ground-state HOMOs/LUMOs at the  $S_1$  geometry, see Table S1, Supporting Information).

Selected changes in bond lengths ( $\Delta r$ ) and dihedrals ( $\Delta\phi_i$ ) on going from the ground to the excited states are shown in Figure 3 for **oP**<sup>4</sup>, **oP**<sup>6</sup>, and **oP**<sup>8</sup>. As would be expected on the basis of the known planarization of biphenyl (**oP**<sup>2</sup>) and *para*-phenylenes on excitation,<sup>22</sup> the torsional angles ( $\phi_i$ ) along the backbone of the *ortho*-phenylenes decrease significantly in the  $S_1$  state, although complete planarization is obviously prevented by steric interactions ( $\phi_i = 20$ – $30^\circ$  in the excited state, compared to  $\phi_i = 60$ – $65^\circ$  in the ground state). For the longer oligomers (**oP**<sup>6</sup> and **oP**<sup>8</sup>), the  $S_1$  state geometry is desymmetrized as planarization is localized at one end of the molecule.<sup>23</sup> Inspection of the changes in bond lengths ( $\Delta r$ ) indicates that the excited-state structural changes correspond to

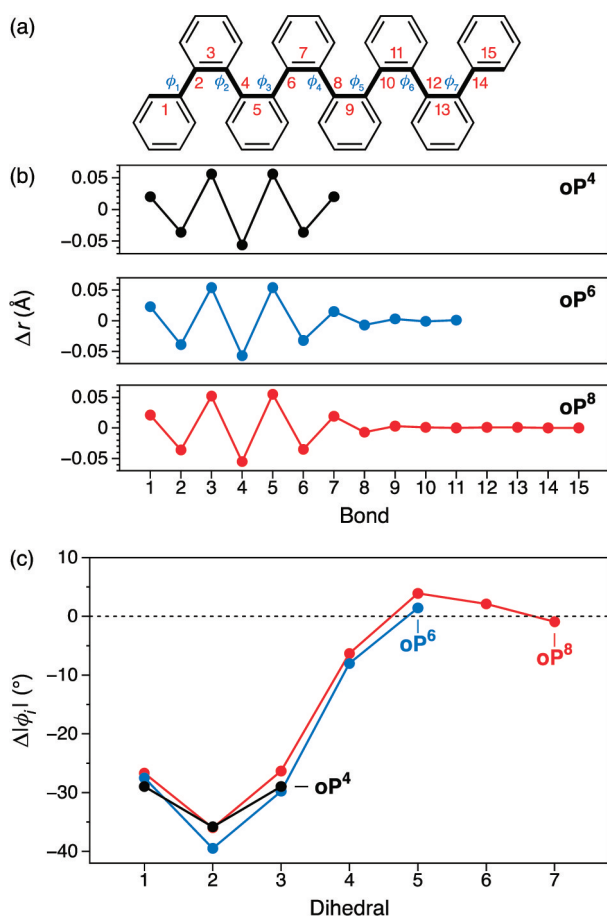


**Figure 3.** (a) Bond and dihedral labeling for  $\text{oP}^8$ . (b) Changes in bond length in the  $S_1$  state (vs  $S_0$ ) for  $\text{oP}^4$ ,  $\text{oP}^6$ , and  $\text{oP}^8$ . (c) Changes in dihedral angle in the  $S_1$  state (vs  $S_0$ ).

*ortho*-quinoid-like structures with significantly shorter biaryl bonds. Both  $\Delta r$  and  $|\Delta\phi_i|$  indicate that the structural perturbations of the excited state extend over roughly four aromatic rings. The frontier molecular orbitals at the  $S_1$  state geometries are localized at the structural distortions (Figure S3, Supporting Information).

The calculated excited-state geometries allow us to rationalize the experimentally observed hypsochromic shifts in fluorescence spectra with increasing oligomer length (for  $n \geq 4$ ). At the ground-state geometries, the HOMO–LUMO gap shows a small decrease with increasing  $n$ , as would be expected for a (weakly) conjugated system and consistent with the short effective conjugation length determined experimentally and reproduced in the calculations (see Table S2, Supporting Information). Conversely, at the optimized excited-state geometries, the HOMO–LUMO gap increases slightly with increasing length for  $n \geq 4$ . The TD-DFT calculations confirm that emission corresponds entirely to a transition between these orbitals. We believe that the trend in fluorescence energies can be explained by inspection of the geometric changes in Figure 3. Excitation corresponds to a compression of these spring-like structures. For the short oligomers ( $n \leq 5$ ), this compression is symmetrically distributed throughout the entire molecule. For the longer oligomers ( $n \geq 6$ ), the structural distortions occur at the ends of the chains, where there will be comparatively less steric strain; in both the ground and excited states, the first two rings at the end of the chain are closer to coplanarity (e.g.,  $\phi_1 =$

$49^\circ$  vs  $\phi_2 = 63^\circ$  for ground-state  $\text{oP}^4$ ). As the length of the oligomer increases, the strain near the structural distortion increases as a greater number of aromatic rings further along the oligomer must twist to accommodate it. For example, note that  $\phi_5$  and  $\phi_6$  for  $\text{oP}^8$  are actually increased (i.e., further from coplanarity) in the excited state (Figure 3c). Thus, the fluorescence energy increases for the longer oligomers as they are sterically less able to accommodate the excited-state structural rearrangements. The length scale of this phenomenon is governed by the three-dimensional structure of the compounds (i.e., the helical pitch), and not directly by  $\pi$ -system delocalization, explaining why the fluorescence spectra of the *ortho*-phenylenes are more strongly dependent on length compared to the UV–vis spectra.<sup>24</sup> Thus, the fluorescence behavior of these compounds directly reflects the relationship between their conformational behavior and their electronic structures.

In summary, we have carried out a TD-DFT investigation of the excited-state properties of the series of parent *ortho*-phenylenes  $\text{oP}^n$ . We have found that their UV–vis spectra are well-reproduced by these calculations, including their effective conjugation length. The unusual hypsochromic shift in their fluorescence spectra with increasing length has been explained using optimized excited-state geometries. Excitation leads to a compression of the spring-like compounds that, for the longer oligomers, is localized at one end of the chain. Because of steric strain, the longer oligomers are less able to accommodate this increased excited-state planarization.

## EXPERIMENTAL SECTION

All calculations were performed using Gaussian 09, rev. B.01.<sup>25</sup> All geometry optimizations were carried out using tight convergence criteria (“opt=tight”), using the PBE0 functional (PBE1PBE) and the 6-31+G(d) basis set. All energy minima (including excited states) were verified to have 0 imaginary frequencies by vibrational frequency analysis. Single-point energy calculations were carried out using the 6-311+G(2d,p) basis set. Simulated UV–vis spectra (Figure S2, Supporting Information) were generated with GaussView 5.0.9 and are based on a 0.333 eV peak half-width at half-height. The 24 lowest energy transitions were calculated for  $\text{oP}^2$  and  $\text{oP}^4$ ; 48 transitions were calculated for  $\text{oP}^5$ ,  $\text{oP}^6$ , and  $\text{oP}^8$ . Geometries and orbitals were visualized using VMD 1.9.<sup>26</sup>

## ASSOCIATED CONTENT

### Supporting Information

Supplementary figures, calculated energies and zero-point vibrational energy corrections of all compounds (ground and excited states), Cartesian coordinates of all geometries, and complete ref 25. This material is available free of charge via the Internet at <http://pubs.acs.org>.

## AUTHOR INFORMATION

### Corresponding Author

\*E-mail: [scott.hartley@muohio.edu](mailto:scott.hartley@muohio.edu).

## ACKNOWLEDGMENTS

Support from the National Science Foundation (CHE-0910477) is gratefully acknowledged. Gaussian 09 was purchased with the assistance of the Air Force Office of Scientific Research (FA9550-10-1-0377).

## REFERENCES

- Berresheim, A. J.; Müller, M.; Müllen, K. *Chem. Rev.* **1999**, *99*, 1747–1785.

(2) For early reports of *ortho*-phenylene oligomers, see: (a) Wittig, G.; Lehmann, G. *Chem. Ber.* **1957**, *90*, 875–892. (b) Ozasa, S.; Fujioka, Y.; Fujiwara, M.; Ibuki, E. *Chem. Pharm. Bull.* **1980**, *28*, 3210–3222. (c) Blake, A. J.; Cooke, P. A.; Doyle, K. J.; Gair, S.; Simpkins, N. S. *Tetrahedron Lett.* **1998**, *39*, 9093–9096.

(3) Tour, J. M. *Adv. Mater.* **1994**, *6*, 190–198.

(4) Ohta, E.; Sato, H.; Ando, S.; Kosaka, A.; Fukushima, T.; Hashizume, D.; Yamasaki, M.; Hasegawa, K.; Muraoka, A.; Ushiyama, H.; Yamashita, K.; Aida, T. *Nature Chem.* **2011**, *3*, 68–73.

(5) He, J.; Crase, J. L.; Wadumethrige, S. H.; Thakur, K.; Dai, L.; Zou, S.; Rathore, R.; Hartley, C. S. *J. Am. Chem. Soc.* **2010**, *132*, 13848–13857.

(6) Hartley, C. S.; He, J. *J. Org. Chem.* **2010**, *75*, 8627–8636.

(7) Mathew, S. M.; Hartley, C. S. *Macromolecules* **2011**, No. 10.1021/ma201866p.

(8) *para*-Phenylenes have much longer effective conjugation lengths of  $n_{\text{ecl}} \approx 10$ : Grimsdale, A. C.; Müllen, K. *Adv. Polym. Sci.* **2006**, *199*, 1–82.

(9) Hypsochromic shifts in absorption spectra have been observed for conjugated oligomers with donor–acceptor substitution. See, for example: Meier, H.; Mühling, B.; Kolshorn, H. *Eur. J. Org. Chem.* **2004**, 1033–1042.

(10) Gierschner, J.; Cornil, J.; Egelhaaf, H.-J. *Adv. Mater.* **2007**, *19*, 173–191.

(11) Pogantsch, A.; Heimel, G.; Zojer, E. *J. Chem. Phys.* **2002**, *117*, 5921–5928.

(12) Yang, L.; Ren, A.-M.; Feng, J.-K.; Wang, J.-F. *J. Org. Chem.* **2005**, *70*, 3009–3020.

(13) Lukeš, V.; Aquino, A. J. A.; Lischka, H.; Kauffmann, H.-F. *J. Phys. Chem. B* **2007**, *111*, 7954–7962.

(14) Lukeš, V.; Šolc, R.; Barbatti, M.; Elstner, M.; Lischka, H.; Kauffmann, H.-F. *J. Chem. Phys.* **2008**, *129*, 164905.

(15) Adamo, C.; Barone, V. *J. Chem. Phys.* **1999**, *110*, 6158–6170.

(16) Kamya, P. R. N.; Muchall, H. M. *J. Phys. Chem. A* **2008**, *112*, 13691–13698.

(17) Jacquemin, D.; Perpète, E. A.; Ciofini, I.; Adamo, C. *Acc. Chem. Res.* **2009**, *42*, 326–334.

(18) Meier, H.; Stalmach, U.; Kolshorn, H. *Acta Polym.* **1997**, *48*, 379–384.

(19) A reviewer pointed out that biphenyl ( $\text{oP}^2$ ) should arguably be omitted from Figure 2a, as it does not include *ortho* linkages and is therefore not an *ortho*-phenylene. This point is well-taken; however, the inclusion of  $\text{oP}^2$  is consistent with Meier's original approach to the calculation of  $n_{\text{ecl}}$  (ref 18) and our own experimental results for *ortho*-phenylenes (refs 5, 7). In any event, excluding  $\text{oP}^2$  does not affect our current conclusions ( $n_{\text{ecl}} \approx 5$ ).

(20) Reimers, J. R.; Cai, Z.-L.; Bilić, A.; Hush, N. S. *Ann. N. Y. Acad. Sci.* **2003**, *1006*, 235–251.

(21) Interestingly, attempts to optimize the  $S_1$  state geometry of  $\text{oP}^3$  were unsuccessful, as it essentially undergoes an electrocyclic ring closure during the energy minimization. It is well-known that  $\text{oP}^3$  can be photochemically converted to triphenylene through this mechanism (Kharasch, N.; Alston, T. G.; Lewis, H. B.; Wolf, W. *Chem. Commun.* **1965**, 242–243) this may explain its non-fluorescence and our current results.

(22) Momicchioli, F.; Bruni, M. C.; Baraldi, I. *J. Phys. Chem.* **1972**, *76*, 3983–3990.

(23) In all cases,  $S_1$  state geometry optimization began with the  $C_2$ -symmetric ground state helix and proceeded directly to the geometries reported here.

(24) While fluorescence data are not available for the  $\text{oP}^n$  series beyond  $\text{oP}^8$ , we have reported a series of substituted *ortho*-phenylenes for which changes in fluorescence spectra persist at least to the dodecamer. See ref 5.

(25) Frisch, M. J.; et al. *Gaussian 09*, rev. B.01; Gaussian, Inc.: Wallingford, CT, 2010.

(26) Humphrey, W.; Dalke, A.; Schulten, K. *J. Mol. Graphics* **1996**, *14*, 33–38.